Proceedings of the ASME 2016 37th International Conference on Ocean, Offshore and Arctic Engineering, OMAE2018
June 17-22, 2018, Madrid, Spain

OMAE2018-77873

LOW FREQUENCY EXCITATION AND DAMPING OF FOUR MODUS IN SEVERE SEASTATES WITH CURRENT

Nuno Fonseca
SINTEF Ocean
Trondheim, Norway
nuno.fonseca@sintef.no

Carl Trygve Stansberg
Ctstansberg Marinteknikk
Trondheim, Norway
ctstansberg.marinteknikk@gmail.com

Kjell Larsen
Statoil ASA
Trondheim, Norway
KLARS@statoil.com

Rune Bjørkli
Statoil ASA
Stavanger, Norway
RUNBJO@statoil.com

Tjerand Vigesdal
Statoil ASA
Stavanger, Norway
TJVI@statoil.com

Oddgeir Dalane
Statoil ASA
Stavanger, Norway
ODDD@statoil.com

ABSTRACT

Model tests have been performed with four mobile offshore drilling units (MODUs) with the aim of identifying wave drift forces and low frequency damping. The MODUs configuration is different, namely on the number and diameter of columns, therefore the sample is representative of many of the existing concepts. The model scale is the same as well as the wave and current conditions. The experimental program includes irregular waves with systematic variations of the significant wave height, wave peak period, current velocity and vessel heading.

The test data is post-processed to identify the surge and sway quadratic transfer functions (QTFs) of the slowly varying excitation, together with the linearized low frequency damping. The post-processing applies a nonlinear data analysis technique known as "cross-bi-spectral analysis" to estimate characteristics of second-order (quadratic) responses from the measured motions and undisturbed incident wave elevation. The empirical QTFs are then compared with numerical predictions to conclude on the role of viscous drift and the applicability of Newman's approximation for calculation of drift forces in irregular waves. Finally, the empirical drift forces, empirical low frequency damping coefficients and low frequency motions statistics are compared for the three MODUs to conclude on the relation between the Semi configuration and the low frequency responses.

1 INTRODUCTION

There has been a considerable number of incidents with mooring line failures on Semi-submersibles over the last 15 years. These incidents point to the possibility that mooring lines are overloaded during storms. In fact, several mooring line failures have been reported for North Sea floating structures along the recent years during severe conditions (Kvitrud, 2014). This has uncovered a need to improve methods, procedures and standard industry practice in design prediction of nonlinear wave loadings in high and steep seas.

The larger uncertainty in the prediction of floating structures mooring line tensions in severe seastates arises from the estimation of low frequency motions (Stansberg 2015). Two wave-floater interaction sub-problems require improved modelling: the low frequency excitation and the low frequency damping. For semi-submersibles, linear diffraction potential flow codes underestimate wave drift forces, especially in severe seastates (Stansberg 2001, Stansberg et al. 2015). Conditions with combined waves and current add complexity and increase discrepancies. The main reason for the discrepancies seems to be contributions from viscous drag on the low-frequency excitation. For sufficiently long waves, mean viscous drag force on the columns above the still water level gives a contribution to the drift force (Dev and Pinkster, 1994). Faltinsen (1990) discusses an additional contribution from the horizontal component of normal drag forces on the pontoons. Higher than second order potential flow effects may also play a role.

The EXWAVE Joint Industry Project (JIP) was initiated with the aim of addressing these problems and come up with improved estimation procedures (Fonseca et al. 2016, 2017). A semi-empirical formula previously proposed to correct wave drift force coefficients of Semis in high seastates with current (Stansberg et al. 2015), was improved in EXWAVE and validated by comparison of predictions with model test data for a semi-submersible. An additional effort was initiated by Statoil in 2015 with comprehensive model tests of three additional Semis. The model test program was designed to investigate the hydrodynamic loads governing the low frequency motion responses, namely the low frequency excitation and damping. The model scales are the same for the 4 Semis (1:50), the mooring systems are similar and the environmental conditions are the same. However, the Semis configuration are different, namely in the number, diameter and shape of columns.

The paper presents and discusses wave drift force coefficients identified from the model tests, as well the damping of the low frequency motions. It presents also an assessment of the EXWAVE semi-empirical correction formula by comparisons for different Semi-submersible configurations. Additional results and discussions for three of the Semis is presented by Larsen et al. (2018), together with proposals for correction of the wave drift forces and estimation of the low frequency damping.

2 CASE STUDY

2.1 Semi-submersibles

The four Semi-submersibles considered in the present work represent drilling vessels (MODUs) with different configurations. Figure 1 shows photos of the models (Semi A to Semi D) and Table 1 presents the main characteristics. All Semis have two pontoons, but the number and shape of the columns are different.

Semis A and B have many of columns (12 and 8 respectively) with circular cross sections. The columns diameters are not large and the displacement of A and B is relatively low. Semi C represents a modern design with only four large volume columns with rectangular cross section and two transversal wing pontoons connecting the longitudinal pontoons. The displacement is large for Semi C. Semi D have four columns and an intermediate displacement. Semis A, B and D include braces with circular cross section.
The models were tested for the survival draft.

Table 1: Main particulars of the 4 Semi-submersibles.

Parameter	Unit	Semi A	Semi B	Semi C	Semi D
Number of columns	[-]	12	8	4	4
Type of columns	[-]	circular	circular	square	circ - sqr
Diameter of columns	[m]	7 / 10	7.5 / 9	16 x 18	12.5 x 12.5
Displacement	[t]	26240	25963	54517	39206
Length of pontoons	[m]	112	92.5	114.4	107.5
Breadth outside ponts.	[m]	68	62.2	76.7	81.25
Ponts. depth x breadth	[m]	7 x 13	7.2 x 13.2	9.8 x 16.3	9.5 x 14.3
Draft	[m]	16	17.5	19.15	23.0
Vert. CoG abv. baseline	[m]	21.4	20.65	25.7	23.65

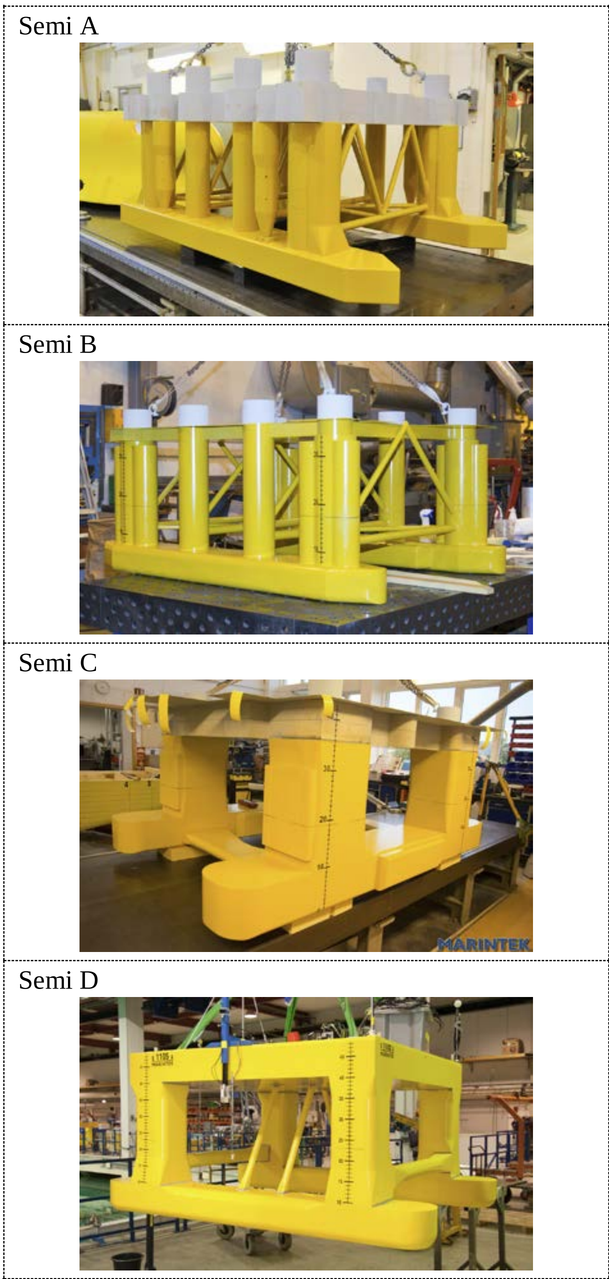

Figure 1: Scaled models of the four Semis (1:50).

2.2 Model tests

Model tests were performed at the Ocean Basin Facility of SINTEF Ocean between October 2015 and March 2016. The model scale is 1:50 for all cases. The aim of the model test programme was to obtain test data to identify the slowly varying wave drift forces, the related wave drift coefficients and slow drift damping. The focus is on the horizontal low frequency motions induced by severe seastates. The wave-current interaction effects on the wave drift forces are also addressed. The tests were performed at 3 m water depth (model scale), which may be considered as deep-water conditions for the wave frequency range of interest.

The vessels were moored with a soft horizontal mooring system with (almost) linear restoring forces in surge, sway and yaw. Table 2 presents some system characteristics identified from pull out tests and decay tests in calm water.

The natural periods of heave and yaw were estimated from the response spectrum peak frequency of tests in irregular waves.

The test matrix includes one small seastate represented by a broad band wave spectrum, one moderate and two severe Torsethaugen seastates. These conditions were repeated for three current velocities (0, 0.82 and 1.58 m/s, collinear waves and current) and for three vessel headings (0, 45 and 90 degrees).

Table 2: System characteristics for the four Semis.

Parameter	Unit	Semi A	Semi B	Semi C	Semi D
Horiz. restoring coeff.	[kN/m]	112	110	160	157
Surge natural period	[s]	109	109	133	117
Sway natural period	[s]	137	133	160	136
Heave natural period*	[s]	19.1	20.8	22.4	22.7
Roll natural period	[s]	35.3	38.2	52.1	52.1
Pitch natural period	[s]	40	39.4	52.7	56.6
Yaw natural period	[s]	61.3	58.0	89.2	80.6

* estimated from the motion response in irregular waves

3 ESTIMATION OF WAVE FORCE QTFs

3.1 Method of identification

The present study follows a method to identify surge and sway wave drift force coefficients from measured vessel responses in irregular waves. A post-processing analysis of the test data is carried out to extract empirical wave drift coefficients making use of a nonlinear data analysis known as "cross-bi-spectral analysis" (CBS) to estimate characteristics of second-order responses represented by Quadratic Transfer Functions – QTFs. Such drift coefficients might include higher-order contributions as well as purely quadratic. While a brief explanation is given in the following paragraphs, details of the method can be found in Stansberg (1997, 2001). The procedure follows two major steps:

(a) First, identify the second order wave exciting force (or moment) signal from the measured low frequency (LF) motion response. One assumes a linear mass-damper-spring system represent the LF motion. The system natural frequency, mass and linear spring constants are known. Decay tests provide information for initial assumption of system damping, which is adjusted through an iterative process. The 2nd order excitation force is the only unknown to be determined.

(b) Second, use the undisturbed incident wave elevation and the estimated 2nd order force, together with cross bi-spectral analysis, to identify the difference frequency wave exciting QTF matrix:

$$H^{(2)}(f_m, f_n) = S_{\zeta\zeta g}(f_m, f_n)/S_{\zeta\zeta}(f_m)S_{\zeta\zeta}(f_n) \qquad (1)$$

where $H^{(2)}(f_m, f_n)$ is the wave drift force coefficient corresponding to the wave frequency pair (f_m, f_n), $S_{\zeta\zeta}(f_m)$ represents the wave spectrum and $S_{\zeta\zeta g}(f_m, f_n)$ is the cross bi-spectrum of the 2nd order excitation with respect to the incident wave elevation.

3.2 Example

The quality of the identified QTF matirx can be assessed by comparing the measured LF motion with the same motion calculated using the linear oscillator together with the wave exciting forces reconstructed from the identified QTF. The comparison is done in terms of time histories and LF spectra. As referred above, besides the excitation, the first step involves one additional unknown, namely the LF damping. For this reason, the QTF estimation follows an iterative process where the damping is systematically adjusted until a good convergence of the measured and reconstructed LF motion spectra is achieved. A linearized form of the LF damping is a result of the identification procedure.

Figures 2 and 3 show one example of comparisons between LF sway motion in 90 degrees waves corresponding to the small seastate for Semi C. The agreement between measured and reconstructed LF motions is quite good, which means the identified QTF is accurate.

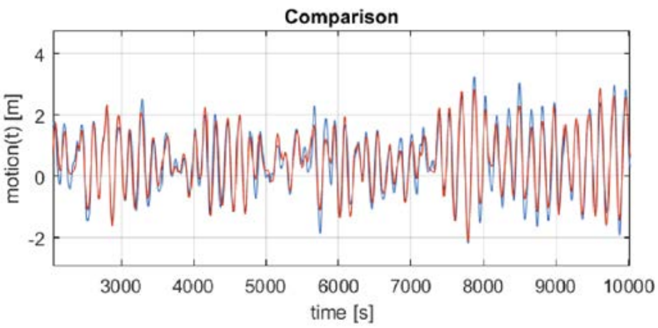

Figure 2: Comparison between measured slow drift sway motion (blue line) and reconstructed from the empirical QTF (red line). Head. = 90 deg., Uc = 0, Hs = 2.5 m, Tp = 5-25 s.

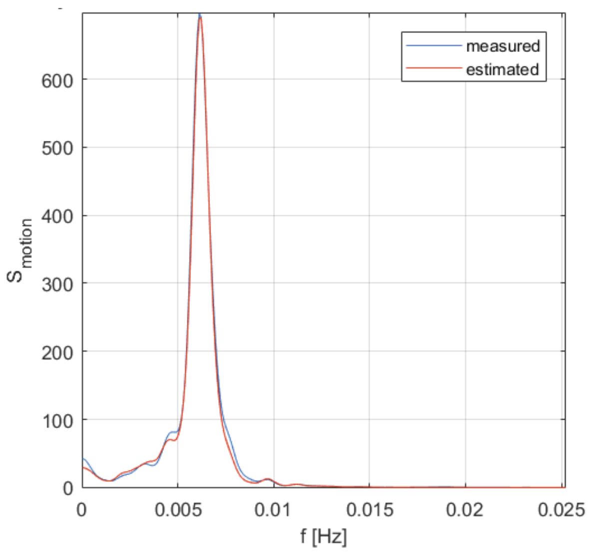

Figure 3: Comparison between experimental (blue) and reconstructed (red) L.F. sway spectra. Head. = 90 deg., Uc = 0, Hs = 2.5 m, Tp = 5-25 s.

3.3 Analysis of full quadratic transfer functions

The method described in the previous Section was applied to identify the difference frequency wave exciting QTFs for the Semis based on the model test data. As an example, Figure 4 shows the surge QTF modulus for Semi A and Semi C identified from the low frequency motions corresponding to a seastate with a significant wave height (Hs) of 11.5 m and wave peak period (Tp) of 12.5 s and no current. The vessel encounters head waves (0 degrees). The wave drift force coefficients are shown as contour plots as function of the bi-frequency in Hz.

The white dashed lines represent coefficients for constant difference frequency. The frequency range along these diagonals is related to the wave spectrum frequency range. The "width" of the identified QTF, or the maximum difference frequency diagonal is related to the low frequency content of the measured response – the vessel does not respond to large difference frequencies, or difference frequencies much larger than the natural period. As an example, Semi A has a surge natural frequency of 0.009 Hz.

The plots of Figure 4 show the force QTFs are different for the two Semis. Observing along the difference frequency diagonals, starting at the low frequency range, the drift forces of Semi C have a much larger first peak than Semi A. This is related to the much larger columns diameter and related diffraction effects which start at lower wave frequencies. Then, as the frequency increases, there is a hallow related to interference effects between the columns, before the drift coefficients increase again. Drift forces are larger for the larger volume structure, which is due to higher diffraction forces.

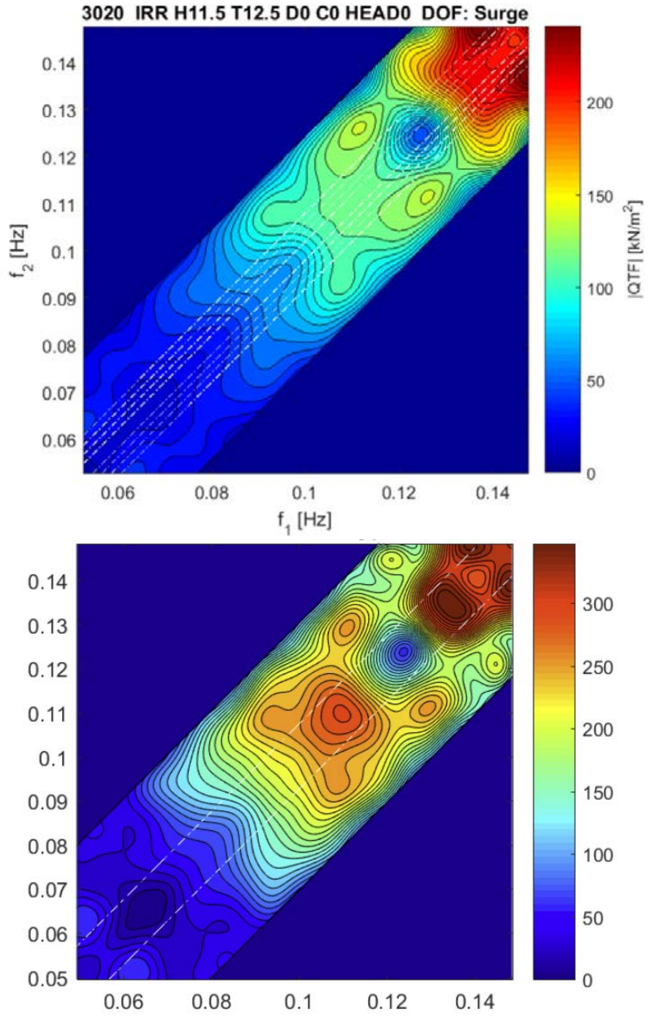

Figure 4: Surge QTF for Semi A (upper graph) and Semi C (lower graph). Head. = 0 deg., Uc=0, Hs=11.5m, Tp = 12.5 s.

Figure 5 repeats the results of the upper plot of Figure 4, but in this case for a seastate with collinear current (Uc) of 0.82 m/s. One observes that the force QTFs are similar, although the case with current shows slightly larger drift forces.

The three plots illustrate one characteristic often observed for the surge and sway force QTFs of Semi-submersibles, namely that the off-diagonal variations of the QTFs around the natural frequency are small. This characteristic explains why usually Newman's approximation to estimate the wave drift forces in irregular waves by using the main QTF diagonal only, often works fine if the natural frequency is low.

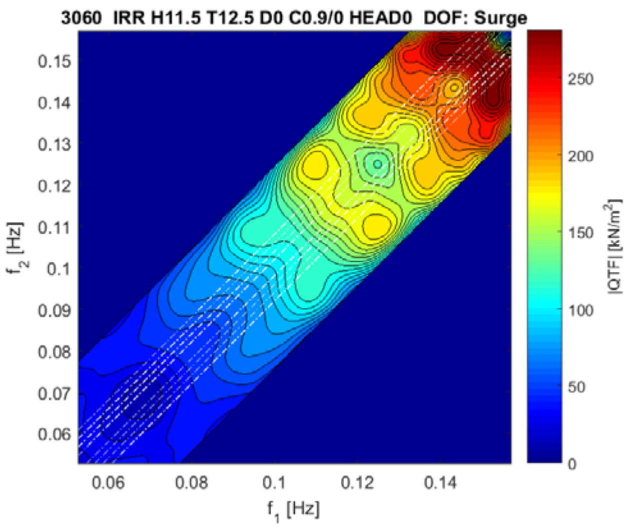

Figure 5: Surge QTF for Semi A. Head. = 0 deg., Uc = 0.82 m/s, Hs = 11.5 m, Tp = 12.5 s.

4 ASSESSMENT OF THE EXWAVE FORMULA

4.1 Diffraction analysis models

Potential flow hydrodynamic coefficients, first order wave exciting forces and mean wave drift forces have been estimated by a 3D linear radiation-diffraction flat panel method (MULDIF, Hermundstad et al. 2016).

4.2 Semi-empirical correction formula

Stansberg at al. (2015) proposed a semi-empirical correction formula to estimate the wave drift force coefficients on column based semi-submersibles. The correction accounts for viscous effects and wave-current interaction effects and it was pointed as a short-term alternative, while more advanced and commonly accepted procedures are not yet in place. Viscous drift forces are particularly important in large seastates and conditions with combined waves and current. The formula has been updated and validated in the scope of Exwave.

The surge/sway wave drift force coefficients for frequency ω and in collinear waves and current (U) conditions is:

$$f_D(\omega, U, H_s) = f_D^{pot}\left(1 + C_p.U.p\right) + B(G.U + H_s)$$

where the first term represents potential flow drift forces including a correction due to wave-current interaction and the second term represents the viscous drift component. Note that the last term including the significant wave height *Hs* is a third order term; i.e. the resulting drift coefficients include a contribution that increases linearly with *Hs*.

Additionally:

- $f_D(\omega, U, H_s) = \frac{F_D(\omega,U,H_s)}{A^2}$ and F_D is the mean wave drift force in harmonic waves with amplitude *A*
- f_D^{pot} is the mean wave drift force coefficients from 1st order potential flow theory with zero current
- C_p is a potential flow wave-current interaction coefficient, assumed as 0.25 s/m
- $p = e^{-0.95(kD_0)^3}$ $[kN/m^3]$ and D_0 is the equivalent main columns diameter.
- $D_0 = \sqrt{4A_{wp}/N\pi}$, A_{wp}= water plane area
- $B = k'.d_{sum}.p$, with $k' = \frac{k}{[1+(k.L)^{-2}]}$
- $k = 2\pi/\lambda$ is the wave number and λ is the wavelength.
- $G = 10\ [s]$ represents a viscous wave-current factor determined empirically.

4.3 Wave drift force coefficients identified from irregular wave tests

The surge wave drift force coefficients corresponding to a small difference frequency (*df*) were extracted from the empirically estimated QTFs and compared to the mean wave drift coefficients from MULDIF and from the Exwave correction formula. Since the slow drift motion spectra have more energy close to the natural frequency (f_n), the most relevant QTF estimates for actual motions are those at difference frequencies around f_n. The identification is assumed more accurate for the frequency range where response spectrum has more energy. For this reason, the procedure consists of extracting a QTF diagonal with *df* between $df = 0$ and $df = f_n$.

Comparing the QTF diagonals described above is valid if the QTF changes slowly around the main diagonal corresponding to $\Delta f = 0$ (which is the same as saying the QTF is nearly constant along diagonals with constant $f_1 + f_2$). Figures 4 and 5 with the empirical QTF shows that in fact the empirical drift coefficients change slowly around the main diagonal.

Figure 6 show comparisons between empirical drift coefficients, MULDIF predictions and Formula results for all the Semis. The force coefficients, which are normalized by the wave amplitude squared, correspond to a small seastate represented by a broadband wave spectrum with Hs = 2.5 m and the wave energy nearly constant between 5 and 25 s. There is no current and the Semis encounter head waves.

There is in general a good agreement between the potential flow predictions and the empirical coefficients, especially for Semis C and D which have larger volume columns. Since the significant wave height for test is small, it is expected that the potential flow results represent correctly the wave drift forces. The fact that the agreement is good indicates the cross bi-spectral analysis method can correctly identify the wave drift force coefficients.

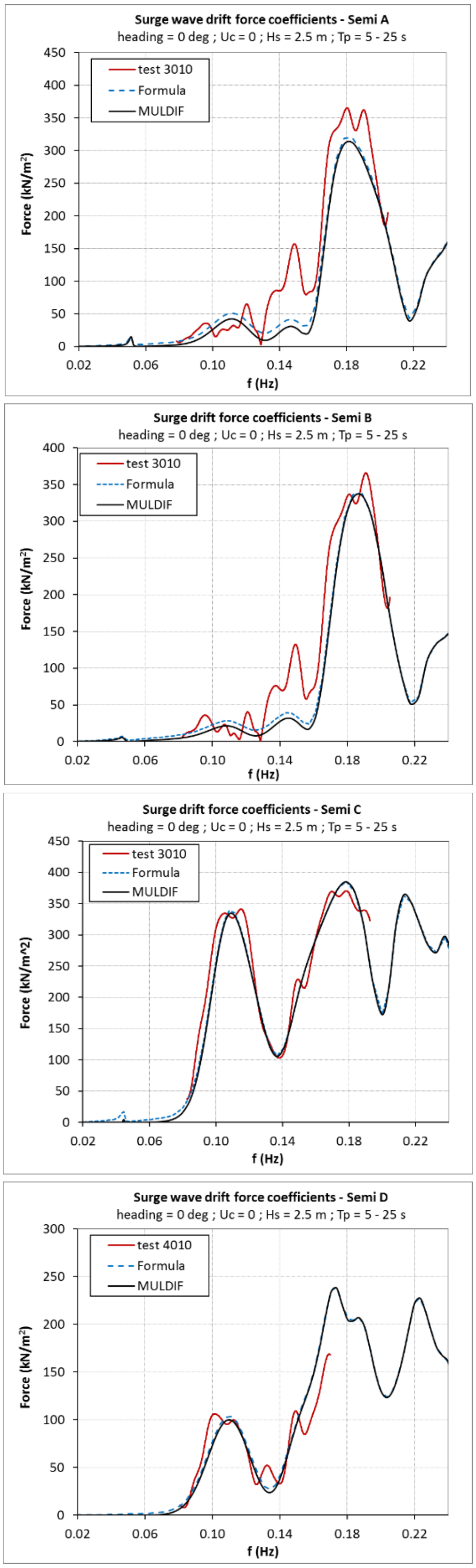

Figure 6: Surge wave drift force coefficients for the four Semis (head. = 0, Uc = 0). Empirical coefficients corresponding to a small seastate represented by a broad band spectrum.

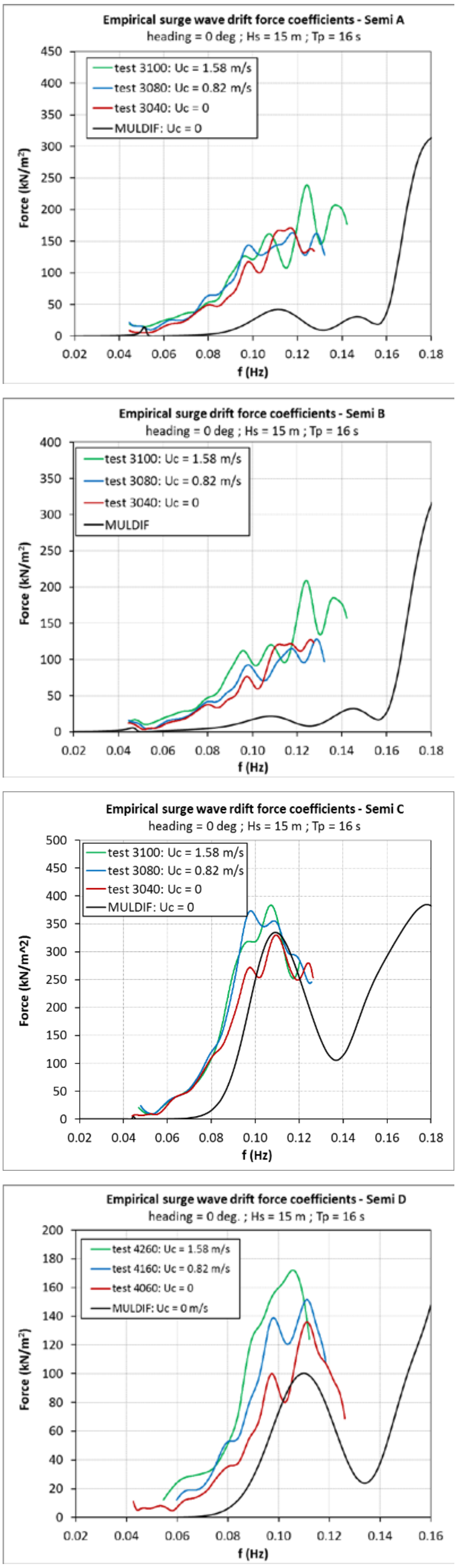

Figure 7: Empirical surge wave drift force coefficients in head waves for all Semis and three current velocities (Hs = 15 m, Tp = 16 s).

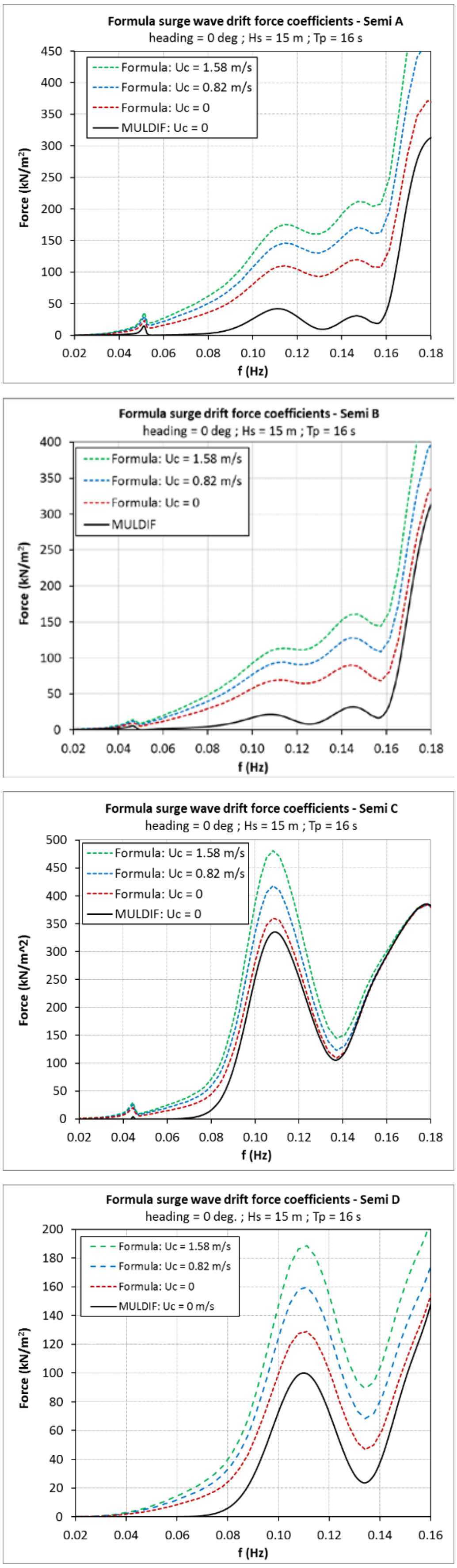

Figure 8: Formula surge wave drift force coefficients in head waves for all Semis and three current velocities (Hs = 15 m, Tp = 16 s).

The agreement is in fact better for cases C and D than for Semis A and B. The latter have a larger number of columns with smaller diameters, therefore diffraction theory is less valid and viscous effects might play a role even in small amplitude waves without current. Discrepancies are observed mainly around 0.14 Hz and the reason is not clear.

Figure 7 and 8 present results like those of Figure 6, but corresponding to a severe seastate with Hs of 15 m and Tp of 16 s and head waves. Each Figure 7 graph shows empirical coefficients for three current velocities (0, 0.82 and 1.58 m/s) together with potential flow predictions for zero current. Figure 8 shows predictions by the Exwave Formula.

Starting with Figure 7, there is a very large underestimation of the wave drift forces of Semis A and B by potential flow predictions for the relevant frequency range, namely between 0.06 and 0.14 Hz. These are the small column diameter Semis and it is obvious that the diffraction method is not valid for the referred frequency range in case of large amplitude waves. Viscous drift dominates in these conditions.

For Semis C and D, with larger diameter columns, diffraction effects are felt above around 0.08-0.09 Hz, but still potential flow predictions underestimate the empirical coefficients between 0.06 and 0.11 Hz. Within this frequency range and for large amplitude waves, the drift forces are given by contribution from both diffraction and viscous effects.

One interesting aspect is the wave-current effects on the empirical drift forces. For Semis C and D the current effects increase the drift forces for frequencies above around 0.08 Hz, especially for the case D. The current effects on the wave drift forces seem to be lower for the Semis A and B with smaller columns diameter.

Comparison of the Exwave semi-empirical Formula predictions with the empirical wave drift coefficients leads to the following conclusions:

- The agreement is between quite good and reasonable, depending of the cases. Predictions are good for the highest current velocity and quite good for Semi D and all current velocities. However, there is a tendency for underestimation for Uc = 0 and 0.82 m/s.
- For Semi C there is underestimation between 0.07 and 0.09 Hz.
- The formula shows a larger effect from the wave-current interactions than that observed for the empirical coefficients.

The potential flow wave drift coefficients presented so far correspond to zero current velocity. However, MULDIF can calculate mean wave drift forces accounting for wave-current interaction effects (likewise to a few other codes). Figure 8 is presented to illustrate the potential flow wave current effects on the surge drift forces. It presents MULDIF and empirical surge wave drift force coefficients for Semi D, the severe seastate (Hs = 15 m, Tp = 16 s) and three current velocities. The results are plotted together with the wave spectrum. The potential flow wave-current effects are significant, but only above around 0.13 Hz, while most of the seastate energy is within 0.03 to 0.10 Hz.

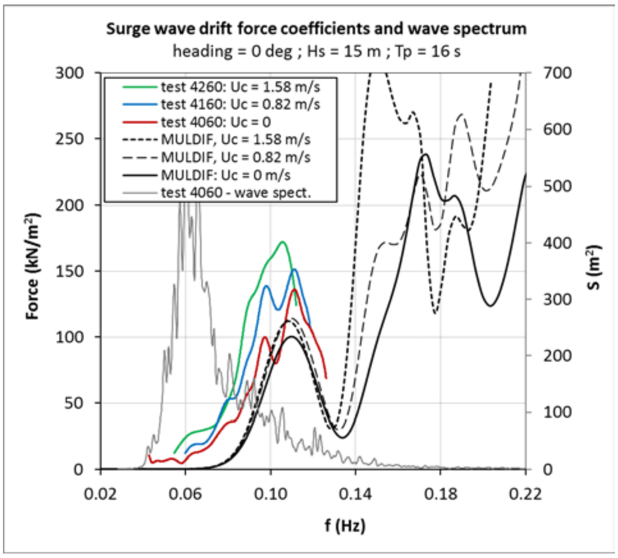

Figure 9: Surge wave drift force coefficients for Semi D in head waves together with the wave spectrum. Hs = 15 m, Tp = 16 s.

5 SLOW DRIFT DAMPING

As explained in Section 3.1, the wave exciting quadratic transfer function estimation from irregular wave tests involves an iterative procedure where a linearized low frequency damping coefficients is adjusted until a good convergence of the measured and reconstructed low frequency (LF) motion spectra is achieved. The identified surge linear damping coefficients are shown in Figure 9 for all the Semis. The results correspond to tests in head waves and the coefficients are presented as a percentage of the critical damping.

The surge LF damping is small for the low seastate without current, at between 3 and 10 % of the critical damping. The damping increases very much with the seastate severity, up to 30 % of the critical damping for conditions without current. The current increases further the LF damping, which in this case achieves 50 % for Semis A and B, 45 % for Semi D and 34 % for Semi C.

One should note that the identified values include the wave drift damping effects (modification of the wave drift forces with the slow drift velocity) and a small contribution from the horizontal mooring lines. Actual mooring systems and dynamic positioning systems will increase further the LF damping of Semi-submersibles, as discussed in Larsen et al. (2018).

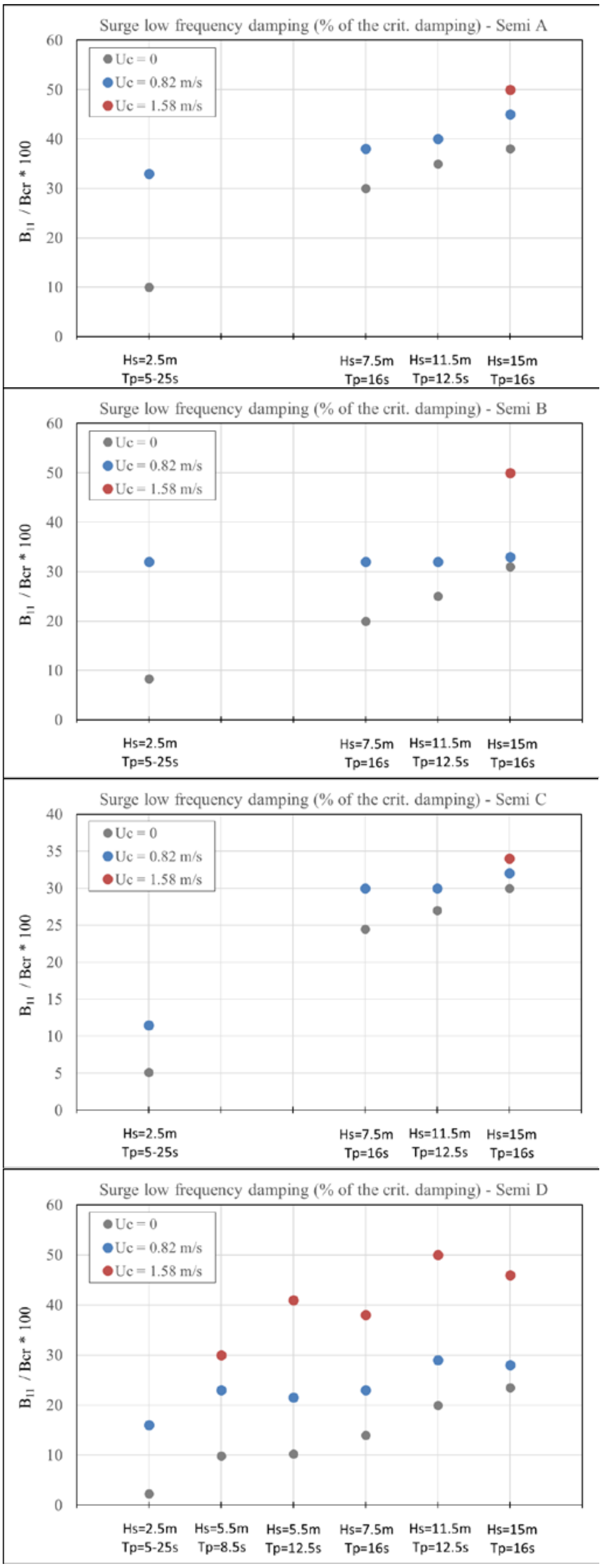

Figure 9: Linearized surge low frequency damping identified from the model tests for all Semis. Head waves and collinear waves and current.

6 CONCLUSIONS

The paper presents and discusses wave drift force coefficients identified from model tests with four different Semi submersibles in severe seastates. Conditions with collinear current are included. The identification applies a second order signal analysis technique based on cross bi-spectral analysis. Good agreement between potential flow drift force coefficients and identified ones in small seastates, for all four Semis, demonstrates that the identification procedure is valid and gives consistent results. It may therefore be applied to identify drift coefficients in high seastates.

The results show large underestimation of the wave drift forces by potential flow predictions at the low frequency range, especially for the Semis with smaller columns diameter. This is due to viscous drift effects. For the two Semis with larger column diameter, the drift forces at the low frequency range results from a combination of potential flow and viscous drift.

Current effects tend to increase the wave drift forces at the low frequency range (between 0.08 and 0.11 Hz). Apparently, the increase is well noticeable for the Semis with larger columns and smaller for the other Semis.

The Exwave semi-empirical formula provides quite good results for conditions with high current (Uc = 1.58 m/s), except for Semi C with the large volume columns. The formula tends to under-predict drift forces for the small current velocities. This is observed for the Semis with small diameter columns (A and B), but also for the Semi with large columns between 0.07 and 0.09 Hz for all currents (C). The agreement is quite good for Semi D.

The surge low frequency damping is small for small seastates without current and it increases very much for high seastates – up to around 30 % of the critical damping. It increases further for conditions with current, reaching 50 % for Uc = 1.58 m/s.

7 ACKNOWLEDGMENTS

The experimental data from Semi D and the related hydrodynamic coefficients were obtained in the in the scope of the EXWAVE JIP and the authors are grateful to the Participants for allowing them to present these results.
The JIP includes the following participants: Bureau Veritas, Deep Sea Mooring, DNV GL, Gusto MSC, Harbin Engineering University, Husky Energy, NOV-APL, NTNU, Odfjell Drilling, Petroleum Safety Authority Norway, Prosafe, Teekay, TU Delft, Samsung Heavy Industries, SBM Offshore, SevanMarine, SINTEF Ocean, Statoil.

8 REFERENCES

Dev, A.K. and Pinkster, J.A., 1994). Experimental evaluation of the viscous contribution to mean drift forces on vertical cylinders. Proceedings, 7th International Conference on the Behaviour of Offshore Structures. (BOSS'94), Massachusetts Institute of Technology, Editor C. Chyssostomidis, Elsevier, Vol. 2, pp. 855 - 875.

Faltinsen, O., 1990. Sea Loads on Ships and Offshore Structures. Cambridge University Press.

Fonseca, N., Stansberg, C.T., Nestegård, Bøckmann, A., Baarholm, R., 2016. The EXWAVE JIP: Improved procedures to calculate slowly varying wave drift forces on floating units in extreme seas. Proc. of the ASME 2016 35th Int. Conf. on Ocean, Offshore and Arctic Eng., June 19-24, 2016, Busan, South Korea, paper OMAE2016-54829.

Fonseca, N. and Stansberg, C.T., 2017. Wave drift forces and low frequency damping on the Exwave Semi-submersible. Proc. of the ASME 2017 36th Int. Conf. on Ocean, Offshore and Arctic Eng., June 25-30, 2017, Trondheim, Norway, paper OMAE2017-62540.

Fonseca, N. and Stansberg, C.T., 2017. Wave drift forces and low frequency damping on the Exwave FPSO. Proc. of the ASME 2017 36th Int. Conf. on Ocean, Offshore and Arctic Eng., June 25-30, 2017, Trondheim, Norway, paper OMAE2017-62540.

Fonseca, N., Ommani, B., Stansberg, C.T., Bøckmann, A., Birknes-Berg, J., Nestegård, A., de Hauteclocque, G., Baarholm, R., 2017. Wave Forces and Low Frequency Drift Motions in Extreme Seas: Benchmark Studies. Proceedings of the Offshore Technology Conference, paper OTC-27803-MS, 1-4 May 2017, Houston, TX, USA.

Hermundstad, E. M., Hoff, J. R., Stansberg, C. T., and Baarholm, R. J., 2016. "Effects of wave-current interaction on floating bodies". In Proc. 35nd Int. Conf. Ocean, Offshore and Arctic Engineering, OMAE2016, June 19-24, Busan, South Korea.

Larsen, K., Bjørkli, R., Vigesdal, T., Dalane, O., 2018. Mooring of semi submersibles in extreme seastates – simplified models for wave drift forces and low frequency damping. Proc. of the ASME 2018 37th Int. Conf. on Ocean, Offshore and Arctic Eng., June 17-22, 2018, Madrid, Spain, paper OMAE2018-77178.

Kvitrud, A, 2014. Lessons learned from Norwegian anchor line failures 2010-2013. Paper OMAE2014-23095, Proc. OMAE2014, San Francisco, Cal., USA, June 2014.

Ommani, B., Fonseca, N. and Stansberg, C.T., 2017. Simulation of low frequency motions in severe seastates accounting for wave-current interaction effects. Proc. of the ASME 2017 36th Int. Conf. on Ocean, Offshore and Arctic Eng., June 25-30, 2017, Trondheim, Norway, paper OMAE2017-62550.

Stansberg, C.T., 1997. Linear and nonlinear system identification in model testing. *International Conference on Nonlinear Aspects of Physical Model Tests*, OTRC, Texas A&M University, College Station, Texas, 2-3 May 1997.

Stansberg, C.T. 2001. Data Interpretation and System Identification in Hydrodynamic Model Testing. *Proc of 11th Int. Offshore and Polar Eng. Conf., ISOPE,* Stavanger, Norway.

Stansberg, C.T., Kaasen, K.E., Abrahamsen, B.C., Nestgåard, A., Shao, Y., Larsen, K., 2015. Challenges in Wave Force Modelling for Mooring Design in High Seas. *Proceedings of the Offshore Technology Conference*, paper OTC-25944-MS, 4-7 May 2015, Houston, TX, USA.

Yang, L., Falkenberg, E., Nestegård, A., Birknes-Berg, J. and Fonseca, N., 2017. Viscous Drift Force and Motions Analysis of Semi-Submersible in Storm Sea States Compared with Model Tests. Proc. of the ASME 2017 36th Int. Conf. on Ocean, Offshore and Arctic Eng., June 25-30, 2017, Trondheim, Norway, paper OMAE2017-62319.